Ultra-Low-Dose Sparse-View Quantitative CT Liver Perfusion Imaging

Esmaeil Enjilela[1], Ting-Yim Lee[1,2], Jiang Hsieh[4], Amol Murjoomdar[3], Errol Stewart[1], Mark Dekaban[1], Feng Su[1], and Aaron So[2]

[1]Imaging Research Laboratories, Robarts Research Institute, London, ON, Canada; [2]Imaging Program, Lawson Health Research Institute, London, ON, Canada; [3]Department of Medical Imaging, Western University, London, ON, Canada; and [4]CT Engineering, GE Healthcare, Waukesha, WI

Corresponding Author:
Aaron So, PhD, FSCCT
Imaging Program, Lawson Health Research Institute,
268 Grosvenor Street, London, ON, Canada, N6A 4V2;
E-mail: aso@robarts.ca

Key Words: sparse-view image reconstruction, compressed sensing, radiation dose reduction, quantitative liver perfusion imaging, hepatic arterial blood flow

Abbreviations: Hepatic arterial blood flow (H_ABF), hepatocellular carcinoma (HCC), dynamic contrast-enhanced (DCE), filtered backprojection (FBP), compressed sensing (CS), computed tomography perfusion (CTP)

ABSTRACT

Radiation dose of computed tomography liver perfusion imaging can be reduced by collecting fewer x-ray projections in each gantry rotation, but the resulting aliasing artifacts could affect the hepatic perfusion measurement. We investigated the effect of projection undersampling on the assessment of hepatic arterial blood flow (H_ABF) in hepatocellular carcinoma (HCC) when dynamic contrast-enhanced (DCE) liver images were reconstructed with filtered backprojection (FBP) and compressed sensing (CS). DCE liver images of a patient with HCC acquired with a 64-row CT scanner were reconstructed from all the measured projections (984-view) with the standard FBP and from one-third (328-view) and one-fourth (246-view) of all available projections with FBP and CS. Each of the 5 sets of DCE liver images was analyzed with a model-based deconvolution algorithm from which H_ABF maps were generated and compared. Mean H_ABF in the tumor and normal tissue measured by the 328-view CS and FBP protocols was within 5% differences from that assessed by the reference full-view FBP protocol. In addition, the tumor size measured by using the 328-view CS and FBP average images was identical to that determined by using the full-view FBP average image. By contrast, both the 246-view CS and FBP protocols exhibited larger differences (>20%) in anatomical and functional assessments compared with the full-view FBP protocol. The preliminary results suggested that computed tomography perfusion imaging in HCC could be performed with 3 times less projection measurement than the current full-view protocol (67% reduction in radiation dose) when either FBP or CS was used for image reconstruction.

INTRODUCTION

There has been considerable improvement in the therapeutic treatments for hepatocellular carcinoma (HCC) and other metastatic diseases in recent years. These advanced therapies require diagnostic and surveillance tools beyond morphology to prevail (1). Quantitative computed tomography perfusion (CTP) can go beyond morphological classification and provide a more accurate tissue characterization via quantitative assessment of hepatic arterial blood flow (H_ABF), which is a useful marker of primary and metastatic hepatic malignancies (1). However, one limitation of the CTP assessment of H_ABF is the higher radiation dose arising from repeatedly scanning the liver after contrast administration (1-3).

Radiation dose reduction for a hepatic CTP study can be achieved by scanning the liver with low x-ray tube current (measured in milliampere) (4, 5). Although the x-ray photon noise in projections can be modeled and corrected for using statistical iterative reconstruction algorithms (6), the dominant electronic noise in very low milliampere conditions cannot be properly modeled with Poisson statistics alone (7), which may lead to poor tumor visualization and inaccurate assessment of hepatic perfusion. Alternatively, dose reduction can be achieved by reducing the number of projections collected in each gantry rotation. However, the aliasing artifact arising from projection undersampling could substantially affect the dynamic contrast-enhanced (DCE) liver images, which could lead to inaccurate hepatic perfusion measurement.

Compressed sensing (CS) was first introduced for signal recovery from underdetermined linear measurements (8) and later exploited for magnetic resonance imaging and computed tomography (CT) reconstruction in sparse sampling conditions (9-12). In this study, we investigated the effectiveness of CS and the conventional filtered backprojection (FBP) for reconstructing DCE-CT images of the liver from a subset of measured projections in an HCC perfusion study, to determine if sparse-view dynamic acquisition and image reconstruction are feasible for ultra-low-dose CT liver perfusion imaging.

ISSN 2379-1381 http://dx.doi.org/10.18383/j.tom.2017.00018

MATERIALS AND METHODS

CS-Based CT Image Reconstruction

CT images are typically smooth except at the boundaries, that is, differences in image values (expressed in Hounsfield units) between adjacent pixels are insignificant, and hence, the first derivative of the images tends to be zero except at the edges where different neighboring materials constitute abrupt changes in image values. This spatial sparsity can be exploited by compressed sensing (CS), where CT image reconstruction is formulated as a constrained optimization problem (12):

$$\min_i \sum_i \|D_i x\|, \text{ s.t. } Ax = p$$

where x is the reconstructed attenuation coefficient, $D_i x$ is the discreet gradient of x, A is the design matrix, p is the measured projection, and $\|.\|$ is the 2-norm. We used the total variation minimization in our CS algorithm to more effectively preserve the edges compared with other available algorithms (12), thus prohibiting the spillover of the high-density regions to adjacent low-density regions. The total variation minimization in the above equation was solved using the augmented Lagrangian multiplier method as described in Li et al.'s study (12).

Data Acquisition and Analysis

The effectiveness of CS and FBP for sparse-view reconstruction of DCE liver images to measure hepatic perfusion was investigated in a clinical HCC CT perfusion study. The patient study was approved by the institution human research ethics review board. Iodinated contrast (Isovue 370) was injected intravenously at 4 mL/s at a dosage of 0.7 mL/kg in a patient weighing 68 kg; a 64-row CT750 HD scanner (GE Healthcare, Waukesha, Wisconsin) was used to acquire DCE liver images. Dynamic scanning of a 75-mm liver section was conducted under 120 kV, 70 mA, and 0.4 seconds of gantry rotation speed by using an axial shuttle mode, in which the scanner table was joggled between 2 adjacent 40-mm sections for 42 times (there was 5-mm overlap between the 2 table positions). The total duration of the imaging study was roughly 2.1 min, and the patient was free breathing throughout the duration. The measured projections were corrected for beam hardening before image reconstruction with FBP and CS.

The following 5 sets of the DCE liver images of 5-mm section thickness were reconstructed using a desktop computer equipped with a 64-GB RAM memory and an Intel(R) Core (TM) i7-3820 3.60 GHz CPU: (a) from all measured projections (984 views per 360°) by using FBP, (b) one-third of projections (328 views) with FBP, (c) one-third of projections with CS, (d) one-fourth of projections (246 views) with FBP, and (e) one-fourth of projections with CS. All the projections used in the sparse-view reconstruction were evenly distributed over 360°. The 328-view (b and c) and 246-view (d and e) protocols used 67% and 75% fewer projections for image reconstruction than the full-view protocol. The corresponding effective doses of the 984-, 328-, and 246-view protocols described above were 11.31, 3.77, and 2.83 mSv, respectively, estimated from the $CTDI_{vol}$ and DLP values reported on the CT750 HD system. Each set of reconstructed DCE liver images was manually registered with the Analyse 10.0 software (Analyze Direct, Overland Park, Kansas) and analyzed with the CT Perfusion software (GE Healthcare) to generate $H_A BF$ maps by use of a model-based deconvolution algorithm (13).

The effectiveness of each sparse-view protocol (b to e) was evaluated on the basis of the $H_A BF$ measurement and tumor visualization with respect to the full-view FBP protocol. In particular, mean $H_A BF$ values of the tumor and normal liver tissue measured by using each sparse-view $H_A BF$ map were compared with those acquired by using the full-view $H_A BF$ maps. In addition, the average of all the DCE liver images in each section from each protocol was calculated to generate an average image. The tumor diameters measured by using the average images were compared among the 5 protocols.

RESULTS

Figure 1A–C shows the average liver images that correspond to the full-view (984-view) FBP (Figure 1A), sparse-view (328-view) FBP (Figure 1B), and sparse-view CS (Figure 1C) protocols. The 328-view FBP and CS average images were comparable with the reference full-view FBP average image in terms of anatomical details, as the diameter of the liver tumor measured by using each average image was 1.39 cm.

Figure 2, A–C shows the $H_A BF$ maps acquired by the same protocols as in Figure 1. The mean $H_A BF$ value in the tumor region measured by using the full-view FBP $H_A BF$ map was 59.8 ± 14.1 mL/min/100*g* (Figure 2A), which was within 2.6% and 0.7% of the mean $H_A BF$ value measured by using the 328-view FBP $H_A BF$ map (61.4 ± 15.0 mL/min/100*g*; Figure 2B) and the 328-view CS $H_A BF$ map (59.4 ± 14.8 mL/min/100*g*; Figure 2C), respectively. A similar agreement in $H_A BF$ measurement was observed in the adjacent normal tissue region: 26.0 ± 8.2 mL/min/100*g* from full-view FBP (Figure 2A) compared with 24.8 ± 5.1 mL/min/100g from the 328-view FBP (Figure 2B) and 25.6 ± 12.1 mL/min/100*g* from the 328-view CS (Figure 2C).

When the number of projection views further reduced to 246 (extremely sparse-view condition), both FBP and CS reconstruction manifested larger anatomical and functional discrepancies with respect to the full-view FBP scheme. The tumor diameter measured by using the 246-view FBP and CS average images was 1.06 cm (Figure 1D) and 1.13 cm (Figure 1E), respectively, which were 26.9% and 20.6% smaller than that measured by using the 984-view FBP average image (1.39 cm; Figure 1A). With regard to $H_A BF$ measurement, the 246-view FBP and CS protocols overestimated $H_A BF$ in the normal liver region by 26% (32.7 ± 22.8 mL/min/100*g*) and 35% (35.1 ± 25.4 mL/min/100*g*), respectively, relative to the full-view FBP protocol (26.0 ± 8.2 mL/min/100*g*). By contrast, differences in $H_A BF$ in the tumor region were <5% among the 3 protocols, as follows: 57.7 ± 33.4 mL/min/100*g* from 246-view FBP versus 56.9 ± 16.2 from 246-view CS versus 59.8 ± 14.1 mL/min/100*g* from 984-view FBP. Although the mean $H_A BF$ measured from the two 246-view protocols was comparable, the 246-view FBP protocol exhibited a larger standard deviation of the mean compared with the 246-view CS protocol (33.4 vs 16.2 mL/min/100*g*).

The liver in each map is outlined by an orange solid line. All $H_A BF$ maps are displayed with a color scale ranging from 0 to 250 mL/min/100*g*.

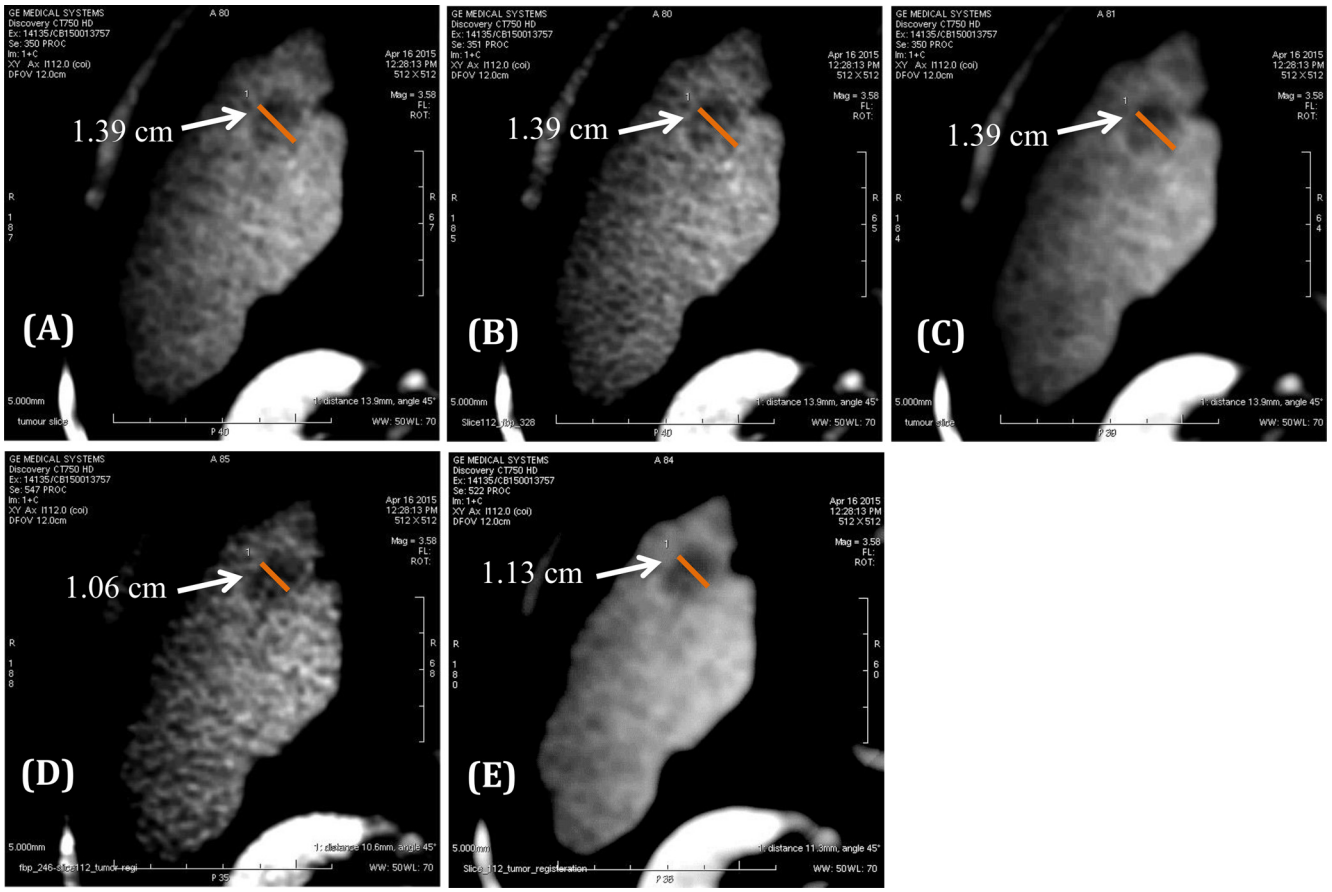

Figure 1. Average dynamic contrast-enhanced (DCE) liver images acquired with different image reconstruction protocols: 984-view FBP (A), 328-view FBP (B), 328-view CS (C), 246-view FBP (D), and 246-view CS (E). All images are displayed with 50 Hounsfield Units (HU) window width and 70HU window level.

DISCUSSION

CT perfusion is a useful tool for quantitative measurement of H_ABF, which is a useful marker of primary and metastatic hepatic malignancies. In this study, we simulated the sparse-view dynamic acquisition for low-dose CT liver perfusion imaging by reconstructing the DCE liver images from an evenly spaced subset of the measured projections. The results from this simulated sparse-view HCC patient study suggested that the H_ABF measured from 328-view dynamic acquisition with either FBP or CS image reconstruction was comparable with that measured from the conventional full-view dynamic acquisition with FBP reconstruction.

Furthermore, the DCE liver images acquired with the 328-view FBP and CS protocols had a slightly smoother appearance compared with those acquired with the full-view FBP; this was because of the regularization applied in the CS algorithm to reduce the streak artifacts arising from sparse projection sampling. Owing to the ill-conditioning of the CT reconstruction, a regularization is necessary to minimize error propagation in the presence of noise during image reconstruction.

Although the edges in the 328-view CS DCE image (Figure 1C) were slightly smoother compared with the reference 984-view FBP DCE image (Figure 1A), the spatial resolution was sufficient to assess the location and extent of the HCC lesion. In our study, the diameter of the tumor lesion measured by using the 328-view CS and 984-view FBP DCE images was identical (1.39 cm). Further, the high resolution of DCE liver images is not necessary for measuring liver perfusion because liver perfusion maps are generated at one-half of the spatial resolution of the source images. This is evident by the example shown in Figure 2, in which the hepatic arterial blood flow maps in Figure 2A–C had comparable perfusion values in the tumor and normal tissue regions. However, further reduction in the number of projections to <328 has led to substantial degradation in the DCE liver images and to inaccurate H_ABF measurement, regardless of whether FBP or CS was used for image reconstruction.

These results have 2 implications—first, the radiation dose of a liver CT perfusion study could be reduced by 67% from the full-view dynamic acquisition protocol without affecting the accuracy of hepatic perfusion measurement. The effective radiation doses of the full-view and the sparse-view protocols for 80-mm coverage of the liver were 11.3 and 3.8 mSv, respectively. Our finding also suggests that the DCE liver images could not be reconstructed with fewer than 328 projections without affecting the image resolution (tumor visualization) and accuracy of the hepatic perfusion measurement. Although additional

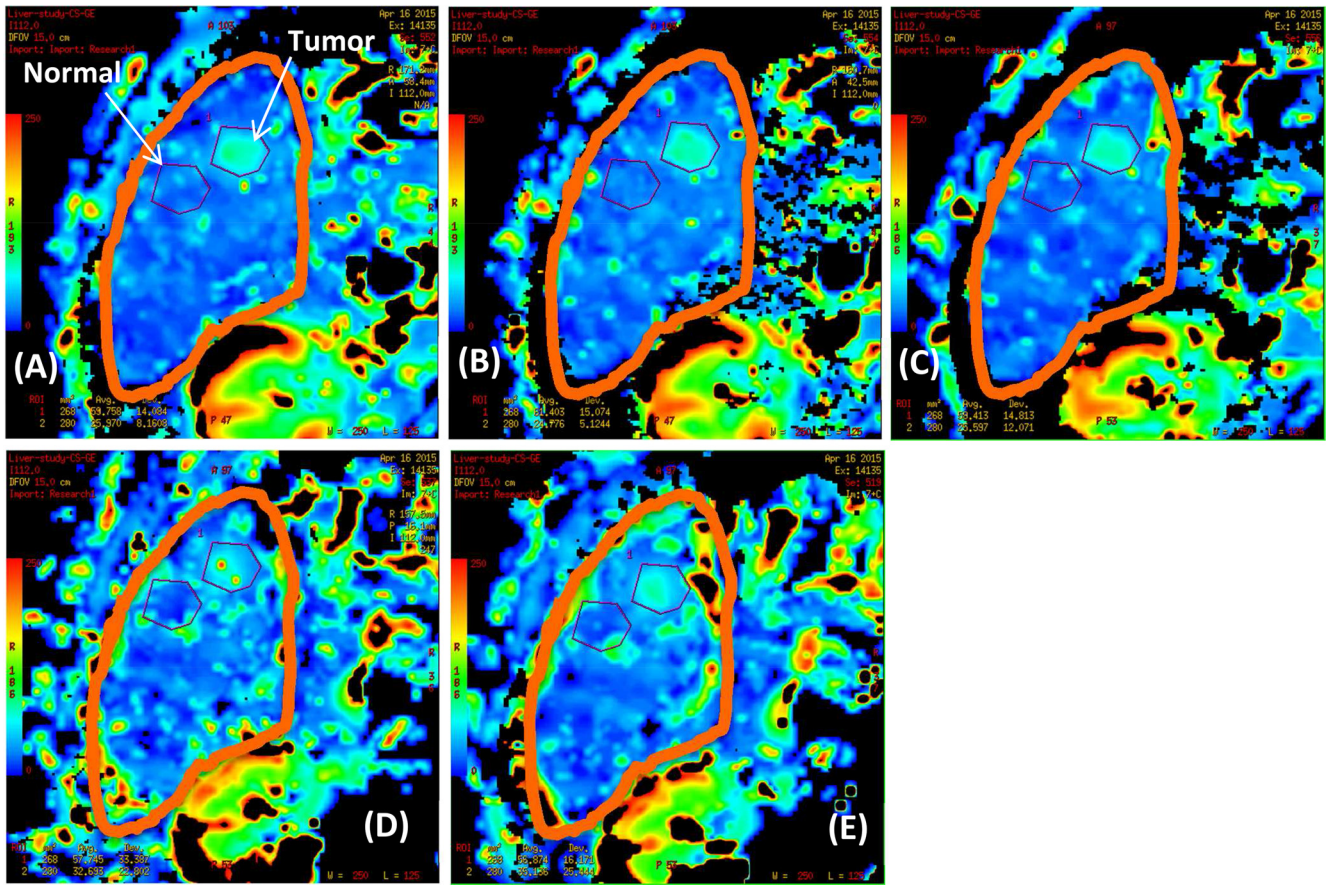

Figure 2. Hepatic arterial blood flow (H_ABF) maps generated from the same sets of DCE images as in Figure 1: 984-view FBP (A), 328-view FBP (B), 328-view CS (C), 246-view FBP (D), and 246-view CS (E). All blood flow maps are displayed with a colour-coded scale ranges from 0 (blue) to 250 (red) mL/min/100g.

dose reduction could be achieved by reducing the x-ray tube current in conjunction with the sparse-view dynamic acquisition, the increased projection noise may pose challenges to both analytical (FBP) and iterative (CS) image reconstructions, particularly in the sparse sampling condition. Second, the conventional and fast FBP algorithm may be sufficient for the reconstruction of DCE liver images from sparsely sampled projections without the need of CS, which is computationally intensive. The shorter image reconstruction time with FBP may facilitate the clinical implementation of the sparse-view CT liver perfusion imaging.

The computation time required to reconstruct one DCE liver image with CS is about 10 times longer than that required to reconstruct the same with FBP. For the 984-view reconstruction using a desktop computer (the computer specifications have been provided in the main text above), the average time required for FBP and CS to reconstruct one DCE image was 20.4 and 207.6 seconds, respectively; for the 328-view reconstruction, the corresponding time required for FBP and CS to reconstruct one DCE image was 7.1 and 69.2 seconds, respectively. The process time was roughly linearly proportional to the number of projections used for image reconstruction. It should be noted that all clinical CT systems are equipped with a much more powerful processing unit than our desktop computer. Hence, the computation time required for the 328-view CS reconstruction should be much shorter.

Apart from the sparse-view approach, x-ray exposure in quantitative CT-liver perfusion imaging can be decreased by reducing the x-ray photon flux (controlled by the x-ray tube current measured in milliampere) used for scanning. Reducing x-ray tube current in conjunction with sparse projection sampling may further decrease the radiation dose of a CT-liver perfusion imaging study. However, decreasing the tube current may limit the visualization of low-contrast components (5), which can be problematic for quantitative assessment of CT perfusion. Further investigation is needed to determine the effect of low milliampere on sparse-view image reconstruction with CS.

In conclusion, our findings obtained on the basis of the study conducted in a single patient with HCC showed that the diagnostic quality of the liver anatomical images and H_ABF maps acquired with a sparse-view (328-view) dynamic acquisition and reconstruction protocol was not inferior to that acquired with a conventional full-view (984-view) dynamic acquisition and FBP reconstruction protocol. Although the preliminary findings suggested that the proposed sparse-view approach could lead to a substantial dose reduction (up to 67%

lower) compared with the conventional protocol, more HCC studies are needed to confirm the usefulness of the proposed sparse-view approach for low-dose quantitative CT perfusion imaging of the liver.

ACKNOWLEDGMENTS

The authors thank Donna Findlay from St. Joseph's Healthcare London and Anna MacDonald from London Health Sciences Centre for assisting in the patient study; the authors also thank Xiaotian Li from the University of Western Ontario for assisting with image registration required for data analysis.

Disclosures: Ting-Yim Lee licenses the CT Perfusion software to GE Healthcare. Jiang Hsieh is an employee of GE Healthcare. Aaron So receives grant support from the Natural Sciences and Engineering Research Council of Canada. Other authors have no disclosure related to the work discussed in this manuscript.

Conflict of Interest: The authors have no conflict of interest to declare.

REFERENCES

1. Pandharipande PV, Krinsky GA, Rusinek H, Lee VS. Perfusion imaging of the liver: current challenges and future goals. Radiology. 2005;234:661–673.
2. Oğul H1, Kantarcı M, Genç B, Pirimoğlu B, Cullu N, Kızrak Y, Yılmaz O, Karabulut N. Perfusion CT imaging of the liver: review of clinical applications. Diagn Interv Radiol. 2014;20:379–389.
3. Kim SH, Kamaya A, Willmann JK. CT perfusion of the liver: principles and applications in oncology. Radiology. 2014;272(2):322–344.
4. Wang WJ, Zhong L, Hua XL, Fan Y, Li L, Xu JR. Low-dose hepatic computed tomography perfusion imaging and its preliminary study. J Dig Dis. 2011;12:204–209.
5. Negi N, Yoshikawa T, Ohno Y, Somiya Y, Sekitani T, Sugihara N, Koyama H, Kanda T, Kanata N, Murakami T, Kawamitsu H, Sugimura K. Hepatic CT perfusion measurements: A feasibility study for radiation dose reduction using new image reconstruction method. Eur Radiol. 2012;81:3048–3054.
6. Nuyts J De Man B Fessler JA Zbijewski W Beekman FJ. Modelling the physics in iterative reconstruction for transmission computed tomography. Phys Med Biol. 2013;58(12) R63–R96.
7. Xu J, Tsui BM. Electronic noise modeling in statistical iterative reconstruction. IEEE Trans Image Process. 2009;18(6):1228–1238.
8. Candès E, Romberg J, Terence T. Stable signal recovery from incomplete and inaccurate measurements. Comm Pure Appl Math. 2006;59(8):1207–1223.
9. Lustig M, Donoho D, Pauly JM. Sparse MRI: The application of compressed sensing for rapid MR imaging. Magn Reson Med. 2007;58(6):1182–1195.
10. Pan X, Sidky EY, Vannier M. Why do commercial CT scanners still employ traditional, filtered back-projection for image reconstruction? Inverse Probl. 2009; 25(12):1230009.
11. Chen GH, Tang J, Leng S. Prior image constrained compressed sensing (PICCS): a method to accurately reconstruct dynamic CT images from highly undersampled projection data set. Med Phys. 2008;35(2):660–663.
12. Li C, Yin W, Jiang H, Zhang Y. An efficient augmented Lagrangian method with applications to total variation minimization. Comput Optim Appl. 2013;56:507–530.
13. Stewart EE, Chen X, Hadway J, Lee TY. Hepatic perfusion in a tumor model using DCE-CT: an accuracy and precision study. Phys Med Biol. 2008;53(16):4249–4267.